

Resolution dependence of most probable pathways with state-dependent diffusivity

Alice L. Thorneywork,^{1,2} Janes Gladrow,³ Ulrich F. Keyser,²
Michael E. Cates,⁴ Ronojoy Adhikari,⁴ and Julian Kappler^{4,5}

¹*Physical and Theoretical Chemistry Laboratory, University of Oxford,
South Parks Rd, Oxford OX1 3QZ, United Kingdom*

²*Cavendish Laboratory, University of Cambridge,
J J Thomson Ave, Cambridge CB3 0HE, United Kingdom*

³*Microsoft Research, Station Rd, Cambridge CB1 2FB, United Kingdom*

⁴*Department of Applied Mathematics and Theoretical Physics,
Centre for Mathematical Sciences, University of Cambridge,
Wilberforce Rd, Cambridge CB3 0WA, United Kingdom*

⁵*Arnold Sommerfeld Center for Theoretical Physics (ASC), Department of Physics,
Ludwig-Maximilians Universität München, Theresienstraße 37, D-80333 Munich, Germany*

(Dated: February 5, 2024)

Recent experiments have probed the relative likelihoods of trajectories in stochastic systems by observing survival probabilities within a tube of radius R in spacetime. We measure such probabilities here for a colloidal particle in a corrugated channel, corresponding to a bistable potential with state-dependent diffusivity. In contrast to previous findings for state-independent noise, we find that the most probable pathway changes qualitatively as the tube radius R is altered. We explain this by computing the survival probabilities predicted by overdamped Langevin dynamics. At high enough resolution (small enough R), survival probabilities depend solely on diffusivity variations, independent of deterministic forces; finite R corrections yield a generalization of the Onsager-Machlup action. As corollary, ratios of survival probabilities are singular as $R \rightarrow 0$, but become regular, and described by the classical Onsager-Machlup action, only in the special case of state-independent noise.

In the study of rare diffusive events it is often of interest to know not only the rate at which an initial state transits to a final state but also the most likely sequence of states that connects the initial and final states [1–8]. Care needs to be taken in the definition of the most probable path, or more generally in the quantification of relative probabilities for pairs of paths, since, a priori, single trajectories in diffusive dynamics have vanishing probability. A natural and experimentally measurable resolution consists, instead, of considering the probability of trajectories to remain within a ball of finite radius R around a smooth path [9–18], which represents a tube in spacetime. The corresponding most probable tube (MPT) can, then, be defined as the path that maximises this sojourn probability between given initial and final states [11]. More generally, ratios of probabilities in tubes of equal radius R can be considered, and the limit $R \rightarrow 0$ (should it exist) can be used to define the relative probabilities of paths. Indeed, in recent experimental work [19], the MPT for diffusion processes with state-independent diffusivity was inferred from measured sojourn probabilities and extrapolated to zero radius. Thus experiments can now provide a direct observational underpinning for previously theoretical constructs, such as the identification of most probable paths (MPPs) as minima of a stochastic action. Indeed, the experiments of Ref. [19] confirmed that, for a colloidal system with Langevin dynamics of state-independent diffusivity, the MPPs minimize the Onsager-Machlup (OM) action. This implies, and the experiments confirm, that the vanishing-radius limit of sojourn probability ratios remains well defined for any pair of tubes.

However, in many physical systems the diffusivity is

state-dependent [20–28]. Examples include colloidal particles that interact hydrodynamically with other particles and container boundaries [25–27], and Brownian particles in thermal gradients [24]. While for these scenarios Dürr and Bach showed mathematically that there exists no functional that describes MPPs [11], several possible stochastic actions have been proposed [10, 12, 15–17, 29–33]. However, hitherto neither the non-existence theorem nor the proposed stochastic actions have been related to experimentally observed finite-temperature diffusive dynamics.

In this paper and the accompanying Ref. [34] we provide this connection, and resolve the seeming contradiction between the Dürr-Bach result [11] and the existence of multiplicative-noise actions [10, 12, 15–17, 29–33, 35]. We consider the sojourn probability for diffusion processes with state-dependent diffusivity, and probe the corresponding MPT experimentally for a colloidal particle in a corrugated microchannel, as a paradigmatic example of physical systems with state-dependent diffusivity. We find that the MPT is determined by a radius-dependent competition between the mean diffusivity along the path and a generalized OM action, which we derive in the accompanying Ref. [34]. Importantly, the latter is only a subdominant contribution to the path-dependence of the sojourn probability, and becomes irrelevant in the single-path limit of asymptotically small radius. We thus demonstrate that there is no simple connection between the multiplicative-noise stochastic actions in the literature and physical MPPs, which experimentally confirms the non-existence theorem [11]. More generally our results demonstrate that ratios of path

probabilities of Langevin dynamics are typically singular, and are finite only when the noise is additive.

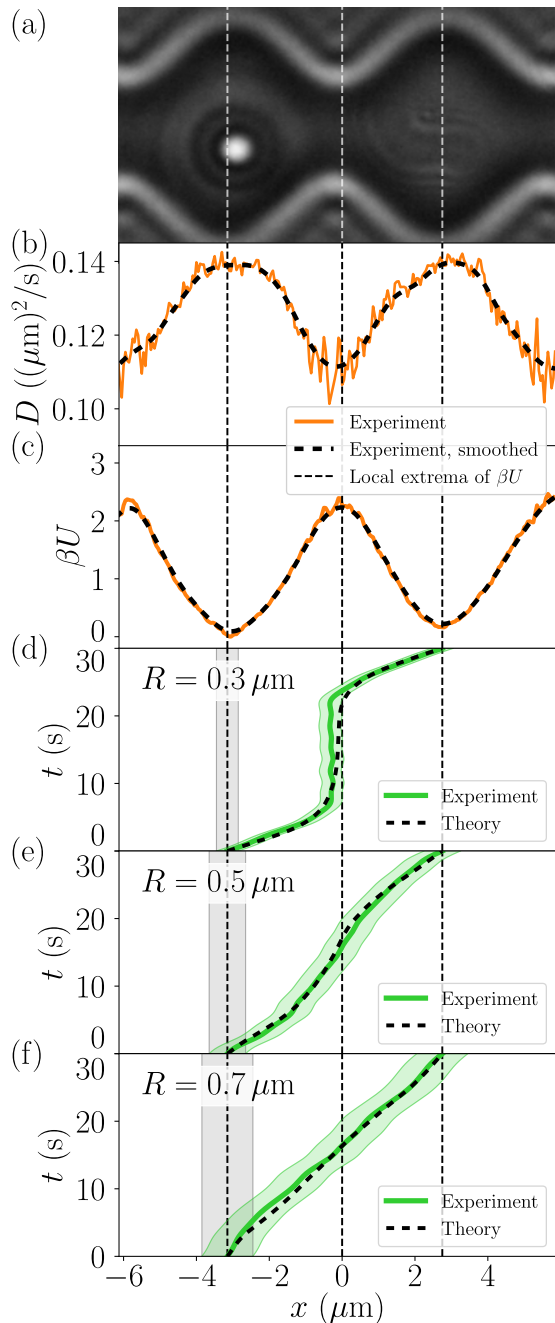


Figure 1. (a) Our experimental setup consists of a colloidal particle in a corrugated channel. (b) Diffusivity and (c) potential profile inferred from recorded time series (orange solid line); black dashed lines are obtained by smoothing using a Hann window average of width $1.5 \mu\text{m}$. (d), (e), (f) Most probable tube (MPT) for barrier crossing for several values of R , inferred from the experimental data via the cloning algorithm from Ref. [19] (green solid lines), and corresponding finite-radius tube (green shaded region). Black dashed lines show theoretical MPT obtained via maximizing Eq. (3) using Eqs. (2), (6); for details see SM [36]. Vertical dotted lines denote local extrema of smoothed potential.

Sojourn probability, tubular stochastic action, and most probable tube. For a smooth reference path φ and tube radius R , we consider the tubular ensemble comprised of all stochastic trajectories that remain within a constant distance R to φ until a final time t_f . The probability that a stochastic trajectory that starts within the tube is still in the tubular ensemble at time t_f is called the sojourn probability $P_R^\varphi(t_f)$.

This probability is equivalently described by the instantaneous exit rate α_R^φ at which stochastic trajectories leave the tube for the first time via [18, 19]

$$P_R^\varphi(t_f) = \exp \left[- \int_0^{t_f} dt \alpha_R^\varphi(t) \right]. \quad (1)$$

We define the negative exponent in this expression as the finite-radius stochastic action functional

$$S_R[\varphi] \equiv -\ln(P_R^\varphi) = \int_0^{t_f} dt \alpha_R^\varphi(t), \quad (2)$$

which fully describes the sojourn probability (modulo dependence on initial conditions, which affect α_R^φ for a short initial duration). From Eq. (2) it is apparent that α_R^φ can be interpreted as a Lagrangian that quantifies sojourn probabilities.

The most probable tube (MPT) for given initial and final positions x_0, x_f , total duration t_f , and tube radius R is defined as

$$\varphi_R^* \equiv \underset{\varphi}{\operatorname{argmin}} S_R[\varphi], \quad (3)$$

where we minimize over paths φ with $\varphi(0) \equiv x_0, \varphi(t_f) = x_f$. According to Eqs. (1), (2), the MPT center φ_R^* maximizes the sojourn probability P_R^φ ; the corresponding tube therefore represents the pathway from x_0 to x_f along which a stochastic trajectory is most likely to remain within a distance R from the reference path.

Experimental setup. In our experiments we consider a colloidal particle moving in a corrugated channel, c.f. Fig. 1 (a). The colloidal system consists of carboxylate functionalised polystyrene particles with diameter $\sigma = 1.2 \mu\text{m}$ in 5mM KCl solution. The microfluidic channel has periodic oscillations in width perpendicular to the channel axis, which vary from approximately 1.6σ to 4.8σ at the narrowest and widest sections of the channel respectively. The height of the channel (perpendicular to the imaging plane) is on the order of the particle diameter and does not vary throughout the design. This results in quasi-two dimensional diffusion of the particle through the channel and approximately flat probability distribution of the particle position in two dimensions. Trajectories are acquired using an automated data acquisition protocol implemented using Holographic Optical Tweezers, as described previously [19, 37].

We record several time series with an observation timestep $\Delta t = 2 \text{ms}$, and retain only the x -component (along the channel axis) to accumulate approximately 6 hours of sample trajectories. By considering only the

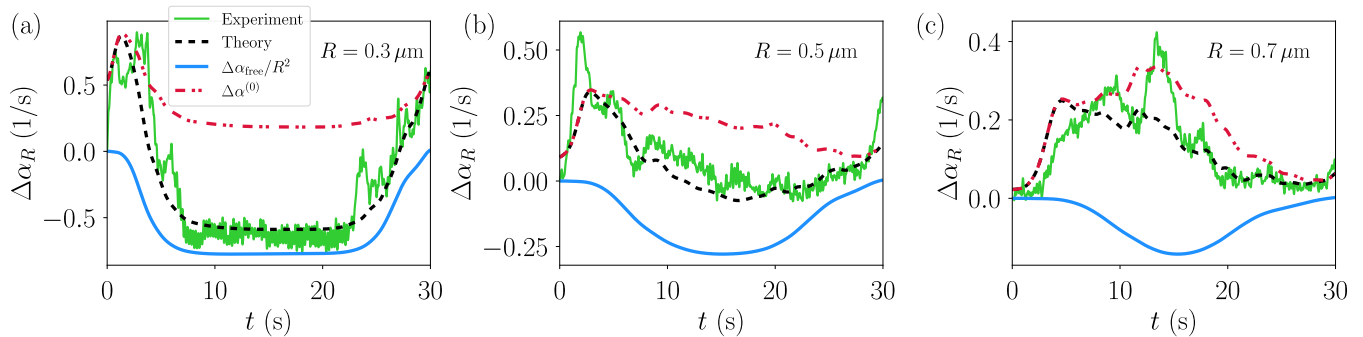


Figure 2. Exit-rate difference Eq. (4) for (a) $R = 0.3 \mu\text{m}$, (b) $R = 0.5 \mu\text{m}$, (c) $R = 0.7 \mu\text{m}$. Green solid line depicts experimental results obtained by directly measuring sojourn probabilities [19, 36]; black dashed line shows analytical results obtained from Eq. (6) using smoothed diffusivity and potential profiles from Fig. 1 (b), (c). Differences in individual terms of Eq. (6) are shown as blue solid and red dash-dotted lines.

x -component of the trajectory, we project the true two-dimensional diffusion onto a one-dimensional description [38, 39]. The varying channel width gives rise to an effective entropic potential, with constrictions acting as entropic barriers. The changing confinement of the particle along the x direction also leads to variation in the effective 1D diffusion coefficient of the particle, which is strongly affected by the variation in hydrodynamic drag arising from differing proximity to the channel walls [40]. As detailed in the SM [36], we estimate the diffusivity and potential profile along the x -direction from our data; we show the resulting profiles in Fig. 1 (b), (c). Figure 1 (a), (b), (c) shows that in regions where the channel has its maximal width, the diffusivity is maximal and the potential landscape features local minima ($x_{\text{left}} \approx -3.2 \mu\text{m}$, $x_{\text{right}} \approx 2.8 \mu\text{m}$). On the other hand, at locations where the channel is most narrow, the diffusivity shows local minima and the potential landscape shows local maxima ($x_{\text{top}} = 0$).

Experimental results. We consider the MPT for a barrier crossing from $x_0 = x_{\text{left}}$ to $x_f = x_{\text{right}}$, and with $t_f = 30$ s. We infer the MPTs from experimental time series using the cloning algorithm from Ref. [19] (for a python implementation, see Ref. [41]). In Fig. 1 we show the resulting experimental MPTs for (d) $R = 0.3 \mu\text{m}$, (e) $R = 0.5 \mu\text{m}$, and (f) $R = 0.7 \mu\text{m}$. From Fig. 1 (d) we observe that for $R = 0.3 \mu\text{m}$ the MPT rests close to the barrier top for about half of the total path duration. This is qualitatively different from the paths in Fig. 1 (e), (f) which cross over the barrier without lingering there.

For the three MPTs, we in Fig. 2 plot the experimentally measured exit-rate difference

$$\Delta\alpha_R(t) \equiv \alpha_R^{\varphi^*}(t) - \alpha_R^\psi(t), \quad (4)$$

between the MPT φ^* and a second path ψ , which rests at the left local minimum x_{left} , as illustrated by gray shaded areas in Fig. 1 (d-f). Since ψ , drift, and diffusivity are independent of time, so is α_R^ψ . Any time-dependence in $\Delta\alpha_R$ thus originates from $\alpha_R^{\varphi^*}$ (in the SM [36] we discuss the advantage of considering Eq. (4) over $\alpha_R^{\varphi^*}$ alone). In

Fig. 2 (a) we see that for $R = 0.3 \mu\text{m}$ the experimental exit-rate difference is negative for times during which the MPT rests close to the barrier top. As such, according to Eq. (4) the exit rate at the minimum x_{left} is larger than at the barrier top. A tube lingering at the potential barrier top is hence more probable than a tube lingering at the potential minimum; we discuss this at first sight counterintuitive result further below. For $R = 0.5 \mu\text{m}$, $R = 0.7 \mu\text{m}$, the exit-rate differences in Fig. 2 (b), (c) are predominantly positive, so that the exit rate along the barrier-crossing tube is larger than at the left minimum.

Theoretical results. To understand the observed crossover from barrier-preferring tubes at small radius to well-preferring tubes at larger radius, we consider a stochastic process X_t described by the Itô equation

$$dX_t = a(X_t)dt + \sqrt{2D(X_t)}dW_t, \quad (5)$$

with drift $a(x)$, state-dependent diffusivity $D(x)$, and increment of the Wiener process dW_t . We note that $a(x)$ is closely related to the spatial derivative of the potential U from Fig. 1 (c), see SM [36] for details. For the dynamics defined by Eq. (5), we in Ref. [34] calculate α_R^φ as power series in the tube radius R , resulting in

$$\alpha_R^\varphi(t) = \frac{\alpha_{\text{free}}^\varphi(t)}{R^2} + \alpha^{\varphi,(0)}(t) + \mathcal{O}(R^2), \quad (6)$$

with

$$\frac{\alpha_{\text{free}}^\varphi(t)}{R^2} = \frac{\pi^2}{4} \frac{D(\varphi(t))}{R^2}. \quad (7)$$

Equation (7) is the steady-state absorbing-boundary exit rate on a domain $[-R, R]$ for diffusive dynamics with a state-independent diffusivity equal to $D(\varphi(t))$ and vanishing drift [18, 34]; we hence call $\alpha_{\text{free}}^\varphi/R^2$ the free-diffusion exit rate.

For small radius Eq. (6) is dominated by the free-diffusion contribution Eq. (7), which depends on $D(\varphi(t))$. For state-dependent diffusivity the exit rate Eq. (6) is thus path-dependent to leading order in the limit $R \rightarrow 0$.

This is the key conceptual difference between sojourn probabilities for multiplicative and additive [18] noise (where D is constant).

The first correction to free diffusion in Eq. (6) is [34]

$$\alpha^{\varphi,(0)} = \frac{1}{4D} (\dot{\varphi} - a)^2 + \frac{1}{2} \partial_x a + \frac{1}{2} \frac{\partial_x D}{D} (\dot{\varphi} - a) \quad (8)$$

$$+ c_1 \frac{(\partial_x D)^2}{D} + c_2 \partial_x^2 D,$$

where drift, diffusivity, and their derivatives, are evaluated along φ , and $c_1 = -(\pi^2 - 3)/16$, $c_2 = (\pi^2 - 6)/24$. Equation (8) is a multiplicative-noise generalization of the OM action [10–12, 15, 17, 18], to which it reduces for state-independent diffusivity. The appeal of our Eq. (8), which is different from the multiplicative-noise Lagrangians in the literature [10–13, 15–17, 33], is its direct relation to the physical observable Eq. (6).

In Fig. 1 (d), (e), (f) and Fig. 2 we show theoretical MPTs and corresponding exit-rate differences. For all values of R the theoretical and experimental MPTs in Fig. 1 agree well. While the corresponding theoretical exit rates (black dashed lines in Fig. 2) do not reproduce all small-scale features of the experimental exit rates, they do capture the overall behavior of the latter. In the SM [36] we furthermore evaluate Eq. (6) on the experimental MPT centers and find very good agreement with the corresponding experimental exit rates.

In Fig. 2 we decompose the theoretical exit-rate difference Eq. (4) into $\Delta\alpha_{\text{free}}/R^2 \equiv (\alpha_{\text{free}}^{\varphi} - \alpha_{\text{free}}^{\psi})/R^2$ and $\Delta\alpha^{(0)} \equiv \alpha^{\varphi,(0)} - \alpha^{\psi,(0)}$. Subplot (a) shows that for $R = 0.3 \mu\text{m}$ the exit rate is dominated by the free-diffusion contribution $\Delta\alpha_{\text{free}}/R^2$, which explains why the MPT from Fig. 1 (d) rests at the barrier top: since Eq. (7) is proportional to the diffusivity, the MPT seeks out spatial regions where the diffusivity is minimized, which for our system is close to x_{top} , c.f. Fig. 1 (b). On the other hand, for $R = 0.7 \mu\text{m}$ we see in Fig. 2 (c) that $\Delta\alpha_R$ is dominated by $\Delta\alpha^{(0)}$, so that the MPT is predominantly determined by Eq. (8) as opposed to Eq. (7). In summary, Figs. 1, 2 show that for $R \lesssim 0.7 \mu\text{m}$ the theoretical exit rate Eq. (6) describes the experimental results well, and explains the qualitative change in the MPT observed in Fig. 1 (d), (e), (f) as a radius-dependent competition between the free-diffusion term Eq. (7) and the next-order correction Eq. (8) in the perturbative exit rate Eq. (6).

Radius-dependence of sojourn probability. According to Eq. (1), the difference Eq. (4) quantifies the ratio of sojourn probabilities $P_R^{\varphi^*}/P_R^{\psi} = \exp[-\int_0^{t_f} dt \Delta\alpha_R(t)]$, which we show in Fig. 3 (a) as function of R . For $R = 0.3 \mu\text{m}$ the MPT is three orders of magnitude more probable than the constant tube resting at the potential minimum x_{left} , which in Fig. 2 (a) we explained by the small-radius dominance of $\Delta\alpha_{\text{free}}/R^2$ in Eq. (6), together with the fact that $D(x_{\text{left}}) > D(x_{\text{top}})$. The diverging limit $R \rightarrow 0$ in Fig. 3 (a) originates from the non-zero term $\Delta\alpha_{\text{free}}/R^2$, and illustrates that ratios of path prob-

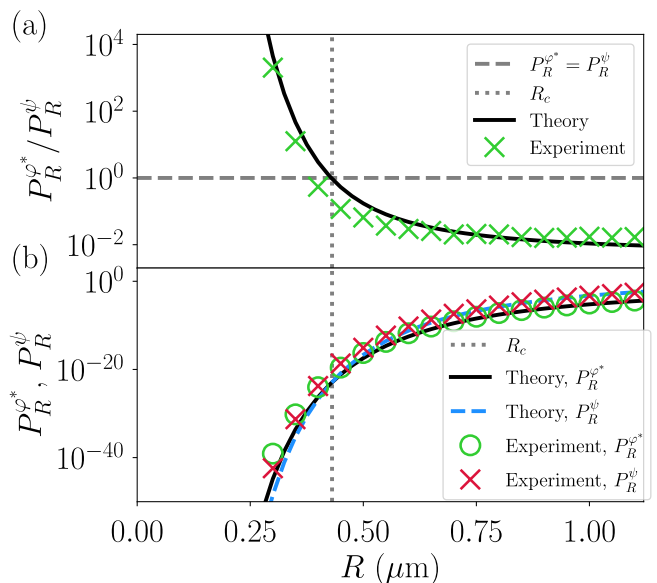


Figure 3. (a) Ratios of sojourn probabilities $P_R^{\varphi^*}/P_R^{\psi}$ for MPT φ^* and path ψ that rests at x_{left} . Green crosses show experimental results, obtained from measured exit-rate differences $\Delta\alpha_R$ via numerical evaluation of $P_R^{\varphi^*}/P_R^{\psi} = \exp[-\int_0^{t_f} dt \Delta\alpha_R(t)]$. Black curves are obtained using the same formula but with perturbative exit rate Eq. (6), and MPTs obtained by minimizing the corresponding theoretical finite-radius action. Horizontal dotted line denotes value $P_R^{\varphi^*}/P_R^{\psi} = 1$. (b) Green and red symbols denote experimental sojourn probabilities $P_R^{\varphi^*}, P_R^{\psi}$ with φ^*, ψ as in (a). Black and orange curves represent the corresponding theoretical sojourn probabilities, evaluated as in (a). Vertical dotted lines in (a), (b) denote the crossover radius $R_c \approx 0.44 \mu\text{m}$ where $P_R^{\varphi^*} = P_R^{\psi}$ (based on theoretical sojourn probabilities).

abilities are in general ill-defined for state-dependent diffusivity. With increasing radius the free-diffusion contribution in Eq. (6) becomes less relevant, and we in Fig. 3 (a) see that at $R_c \approx 0.44 \mu\text{m}$ the barrier-crossing MPT becomes less probable than the tube that rests at x_{left} (in the SM we derive an analytical estimate for R_c [36]).

In Fig. 3 (b) we show $P_R^{\varphi^*}, P_R^{\psi}$ as function of R . For $R = 0.3 \mu\text{m}$ the sojourn probabilities are of the order of 10^{-40} . This emphasizes how rare it is for a stochastic realization at finite temperature to follow a given path closely, and demonstrates the capabilities of our cloning algorithm for probing rare events from data [19, 41]. For small radii $R \lesssim 0.7 \mu\text{m}$ the sojourn probabilities increase steeply with R ; as the free-diffusion term in Eq. (6) becomes less dominant, the slope decreases and the sojourn probabilities approach their asymptotic limit $P \rightarrow 1$ (for $R \rightarrow \infty$).

Conclusions. For a colloidal particle in a corrugated microchannel, we from experimental data infer the most probable tube (MPT) for a barrier crossing with a finite tolerance R for digression from the tube center.

To obtain our results we use a cloning algorithm

[19, 41], which allows us to probe probability distributions on the infinite-dimensional space of all realizations of diffusive dynamics from observed time series.

We find that the MPT is determined by a scale-dependent competition between stochastic and deterministic force, made explicit via the tube radius R in Eq. (6). Intuitively, diffusive stochastic dynamics is for asymptotically small time- and length-scales dominated by random forces, and independent of the deterministic drift. Tubes of asymptotically small radius probe precisely this small-scale behavior [18, 19, 34]. The small-radius limiting MPT therefore first and foremost minimizes the diffusivity along the path. Unless this diffusivity is constant, the MPT minimizes a potential-dependent stochastic action only for sufficiently large tube radius R . We have derived for such cases an action that generalizes the Onsager-Machlup one. While this has a similar form to some previous proposals in the literature [10–13, 15–17, 33], it differs crucially from these in relating experimentally observable quantities, without prior knowledge of the state-dependent diffusivity itself. None of these actions can describe ratios of finite-temperature path probabilities in the experimentally transparent limit where the tube radius $R \rightarrow 0$ (while remaining constant along the path). Instead, as we have shown, this limit is in general singular, with a path that experiences an on average smaller diffusivity being infinitely more probable as compared to a path with on average larger diffusivity.

One consequence of this is that the small-radius MPT

can prefer lingering at potential maxima over minima, c.f. Fig. 1 (d). This challenges the classical view of potential minima as local points of stability, and demonstrates that experimentally observable characteristics of multiplicative noise systems can be radically different from their additive-noise counterparts. Furthermore, our results suggest that for understanding transition pathways in multiplicative-noise systems, focus should be moved from individual paths towards finite-radius tubes, which describe sets of finite probability on the space of all paths.

ACKNOWLEDGMENTS

Work funded in part by the European Research Council under the Horizon 2020 Programme, ERC grant agreement number 740269, and by the Royal Society through grant RP1700. A. L. T. thanks her Royal Society University Research Fellowship. J. G. and U. F. K. were supported by the European Union’s Horizon 2020 research and innovation program under European Training Network (ETN) Grant No. 674979-NANOTRANS. U. F. K. acknowledges funding from an European Research Council Consolidator Grant (DesignerPores 647144). J. K. acknowledges funding from the European Union’s Horizon 2020 research and innovation programme under the Marie Skłodowska-Curie grant agreement No 101068745.

-
- [1] M. I. Dykman, P. V. E. McClintock, V. N. Smelyanski, N. D. Stein, and N. G. Stocks, “Optimal paths and the prehistory problem for large fluctuations in noise-driven systems,” *Physical Review Letters* **68**, 2718–2721 (1992).
 - [2] D G Luchinsky, P V E McClintock, and M I Dykman, “Analogue studies of nonlinear systems,” *Reports on Progress in Physics* **61**, 889–997 (1998).
 - [3] Weinan E, Weiqing Ren, and Eric Vanden-Eijnden, “String method for the study of rare events,” *Physical Review B* **66**, 052301 (2002).
 - [4] Weiqing Ren, Eric Vanden-Eijnden, Paul Maragakis, and Weinan E, “Transition pathways in complex systems: Application of the finite-temperature string method to the alanine dipeptide,” *The Journal of Chemical Physics* **123**, 134109 (2005).
 - [5] Weinan E, Weiqing Ren, and Eric Vanden-Eijnden, “Transition pathways in complex systems: Reaction coordinates, isocommittor surfaces, and transition tubes,” *Chemical Physics Letters* **413**, 242–247 (2005).
 - [6] H. B. Chan, M. I. Dykman, and C. Stambaugh, “Paths of Fluctuation Induced Switching,” *Physical Review Letters* **100** (2008), 10.1103/PhysRevLett.100.130602.
 - [7] Hiroshi Fujisaki, Motoyuki Shiga, and Akinori Kidera, “Onsager–Machlup action-based path sampling and its combination with replica exchange for diffusive and multiple pathways,” *The Journal of Chemical Physics* **132**, 134101 (2010).
 - [8] Timo Schorlepp, Tobias Grafke, and Rainer Grauer, “Gel’fand-Yaglom type equations for calculating fluctuations around instantons in stochastic systems,” *Journal of Physics A: Mathematical and Theoretical* **54**, 235003 (2021).
 - [9] A D Ventsel’ and M I Freidlin, “On small random perturbations of dynamical systems,” *Russian Mathematical Surveys* **25**, 1–55 (1970).
 - [10] Ruslan Leontievich Stratonovich, “On the probability functional of diffusion processes,” *Selected Trans. in Math. Stat. Prob* **10**, 273 (1971).
 - [11] Detlef Dürr and Alexander Bach, “The Onsager-Machlup function as Lagrangian for the most probable path of a diffusion process,” *Communications in Mathematical Physics* **60**, 153–170 (1978).
 - [12] Y. Takahashi and S. Watanabe, “The probability functionals (Onsager-machlup functions) of diffusion processes,” in *Stochastic Integrals*, Vol. 851, edited by David Williams (Springer Berlin Heidelberg, Berlin, Heidelberg, 1981) pp. 433–463.
 - [13] W. Horsthemke and A. Bach, “Onsager-Machlup Function for one dimensional nonlinear diffusion processes,” *Zeitschrift für Physik B Condensed Matter and Quanta* **22**, 189–192 (1975).
 - [14] Ofer Zeitouni, “On the Onsager-Machlup Functional of Diffusion Processes Around Non C2 Curves,” *The Annals of Probability* **17**, 1037–1054 (1989).
 - [15] H. Ito, “Probabilistic Construction of Lagrangean of Diffusion Process and Its Application,” *Progress of Theoret-*

- ical Physics **59**, 725–741 (1978).
- [16] Takahiko Fujita and Shin-ichi Kotani, “The Onsager-Machlup function for diffusion processes,” *Journal of Mathematics of Kyoto University* **22**, 115–130 (1982).
- [17] Nobuyuki Ikeda and Shinzo Watanabe, *Stochastic differential Equations and diffusion processes*, 2nd ed., North-Holland mathematical Library No. 24 (North-Holland [u.a.], Amsterdam, 1989) oCLC: 20080337.
- [18] Julian Kappler and Ronojoy Adhikari, “Stochastic action for tubes: Connecting path probabilities to measurement,” *Physical Review Research* **2** (2020), 10.1103/PhysRevResearch.2.023407.
- [19] Jannes Gladrow, Ulrich F. Keyser, R. Adhikari, and Julian Kappler, “Experimental Measurement of Relative Path Probabilities and Stochastic Actions,” *Physical Review X* **11**, 031022 (2021).
- [20] Nico G. van Kampen, *Stochastic processes in physics and chemistry*, 3rd ed., North-Holland personal library (Elsevier, Amsterdam ; Boston, 2007) oCLC: ocm81453662.
- [21] Gerhard Hummer, “Position-dependent diffusion coefficients and free energies from Bayesian analysis of equilibrium and replica molecular dynamics simulations,” *New Journal of Physics* **7**, 34–34 (2005).
- [22] Felix Sedlmeier, Yann von Hansen, Liang Mengyu, Dominik Horinek, and Roland R. Netz, “Water Dynamics at Interfaces and Solutes: Disentangling Free Energy and Diffusivity Contributions,” *Journal of Statistical Physics* **145**, 240–252 (2011).
- [23] Alexander Berezhkovskii and Attila Szabo, “Time scale separation leads to position-dependent diffusion along a slow coordinate,” *The Journal of Chemical Physics* **135**, 074108 (2011).
- [24] Stefano Bo, Soon Hoe Lim, and Ralf Eichhorn, “Functionals in stochastic thermodynamics: how to interpret stochastic integrals,” *Journal of Statistical Mechanics: Theory and Experiment* **2019**, 084005 (2019).
- [25] T. J. Murphy and J. L. Aguirre, “Brownian Motion of N Interacting Particles. I. Extension of the Einstein Diffusion Relation to the N-Particle Case,” *The Journal of Chemical Physics* **57**, 2098–2104 (1972).
- [26] Gerald Wilemski, “On the derivation of Smoluchowski equations with corrections in the classical theory of Brownian motion,” *Journal of Statistical Physics* **14**, 153–169 (1976).
- [27] Rajesh Singh and R. Adhikari, “Fluctuating hydrodynamics and the Brownian motion of an active colloid near a wall,” *European Journal of Computational Mechanics* **26**, 78–97 (2017).
- [28] Yongge Li, Ruoxing Mei, Yong Xu, J̄ÄErgen Kurths, Jinqiao Duan, and Ralf Metzler, “Particle dynamics and transport enhancement in a confined channel with position-dependent diffusivity,” *New Journal of Physics* **22**, 053016 (2020).
- [29] Robert Graham, “Path integral formulation of general diffusion processes,” *Zeitschrift für Physik B Condensed Matter and Quanta* **26**, 281–290 (1977).
- [30] F. Langouche, D. Roekaerts, and E. Tirapegui, “Functional integral methods for stochastic fields,” *Physica A: Statistical Mechanics and its Applications* **95**, 252–274 (1979).
- [31] C. Wissel, “Manifolds of equivalent path integral solutions of the Fokker-Planck equation,” *Zeitschrift für Physik B Condensed Matter and Quanta* **35**, 185–191 (1979).
- [32] H. Dekker, “On the path integral for diffusion in curved spaces,” *Physica A: Statistical Mechanics and its Applications* **103**, 586–596 (1980).
- [33] Leticia F Cugliandolo, Vivien Lecomte, and Frédéric van Wijland, “Building a path-integral calculus: a covariant discretization approach,” *Journal of Physics A: Mathematical and Theoretical* **52**, 50LT01 (2019).
- [34] Julian Kappler, Michael E. Cates, and Ronojoy Adhikari, “Sojourn probabilities in tubes and pathwise irreversibility for itô processes,” .
- [35] Thibaut Arnoult De Pirey, Leticia F. Cugliandolo, Vivien Lecomte, and Frédéric Van Wijland, “Path integrals and stochastic calculus,” *Advances in Physics* **71**, 1–85 (2023).
- [36] “The supplemental material contains details on langevin model parametrization from experimental data, the cloning algorithm used for inferring sojourn probabilities and exit rates, as well as further numerical and analytical analysis of our data and algorithms,” .
- [37] Alice L. Thorneywork, Jannes Gladrow, Yujia Qing, Marc Rico-Pasto, Felix Ritort, Hagan Bayley, Anatoly B. Kolomeisky, and Ulrich F. Keyser, “Direct detection of molecular intermediates from first-passage times,” *Science Advances* **6**, eaaz4642 (2020).
- [38] P. Kalinay and J. K. Percus, “Projection of two-dimensional diffusion in a narrow channel onto the longitudinal dimension,” *The Journal of Chemical Physics* **122**, 204701 (2005).
- [39] Kevin D. Dorfman and Ehud Yariv, “Assessing corrections to the Fick–Jacobs equation,” *The Journal of Chemical Physics* **141**, 044118 (2014).
- [40] Xiang Yang, Chang Liu, Yunyun Li, Fabio Marchesoni, Peter Hänggi, and H. P. Zhang, “Hydrodynamic and entropic effects on colloidal diffusion in corrugated channels,” *Proceedings of the National Academy of Sciences* **114**, 9564–9569 (2017).
- [41] Julian Kappler, “Cloning algorithm for measuring rare events from stochastic time series, https://github.com/juliankappler/cloning_algorithm,” .